

cIAP1/TRAF2 interplay promotes tumor growth through the activation of STAT3

Baptiste Dumétier, Aymeric Zadoroznyj, Jean Berthelet, Sébastien Causse, Jennifer Allègre, Pauline Bourgeois, Florine Cattin, Cindy Racoeur, Catherine Paul, Carmen Garrido, et al.

▶ **To cite this version:**

Baptiste Dumétier, Aymeric Zadoroznyj, Jean Berthelet, Sébastien Causse, Jennifer Allègre, et al.. cIAP1/TRAF2 interplay promotes tumor growth through the activation of STAT3. Oncogene, In press, 10.1038/s41388-022-02544-y . hal-03882909

HAL Id: hal-03882909
https://hal.science/hal-03882909

Submitted on 2 Dec 2022

HAL is a multi-disciplinary open access archive for the deposit and dissemination of scientific research documents, whether they are published or not. The documents may come from teaching and research institutions in France or abroad, or from public or private research centers.

L'archive ouverte pluridisciplinaire **HAL**, est destinée au dépôt et à la diffusion de documents scientifiques de niveau recherche, publiés ou non, émanant des établissements d'enseignement et de recherche français ou étrangers, des laboratoires publics ou privés.

cIAP1/TRAF2 interplay promotes tumor growth through the activation of STAT3.

Baptiste Dumétier[1,2*], Aymeric Zadoroznyj[1,2*], Jean Berthelet[1,2,a], Sebastien Causse[1,2], Jennifer Allègre[1,2], Pauline Bourgeois[1,2], Florine Cattin[1,2], Cindy Racoeur[3,4], Catherine Paul[3,4], Carmen Garrido[1,2,5], Laurence Dubrez[1,2.]

[1] Institut National de la Santé et de la Recherche Médicale (Inserm), LNC UMR1231, LabEx LIpSTIC, 21000 Dijon, France; Team with the label of excellence from « la ligue national contre le Cancer »
[2] Université de Bourgogne-Franche-Comté, 21000 Dijon, France
[a] Current address: Olivia Newton-John Cancer Research Institute, Heidelberg, Victoria, Australia
[3] LIIC, EA7269, Université de Bourgogne-Franche-Comté, 21000 Paris, France.
[4] Laboratory of Immunology and Immunotherapy of Cancers, EPHE, PSL Research University, 75000 Paris, France.
[5] Anticancer Center Georges François Leclerc-Unicancer, Dijon, France
* these authors contributed equally to this work
Correspondence: ldubrez@u-bourgogne.fr

Running title: cIAP1-TRAF2 interplay in tumor growth

Statement of Significance: cIAP1/TRAF2 complexes regulates the JAK/STAT3 signaling pathway, which is critical for the tumor-promoting activity of cIAP1.

Keywords: cIAP1/oncogene/STAT3/TRAF2.

Data Availability statement: Figshare DOI https://doi.org/10.6084/m9.figshare.21399906

Competing Interests: The authors declare no competing financial interests

Abstract

Cellular inhibitor of apoptosis-1 (cIAP1) is a signaling regulator with oncogenic properties. It is involved in the regulation of signaling pathways controlling inflammation, cell survival, proliferation, differentiation and motility. It is recruited into membrane-receptor associated signaling complexes thanks to the molecular adaptor TRAF2. However, the cIAP1/TRAF2 complex exists, independently of receptor engagement, in several subcellular compartments. The present work strengthens the importance of TRAF2 in the oncogenic properties of cIAP1. cIAPs-deficient mouse embryonic fibroblasts (MEFs) were transformed using the HRas-V12 oncogene. Re-expression of cIAP1 enhanced tumor growth in a nude mice xenograft model, and promoted lung tumor nodes formation. Deletion or mutation of the TRAF2-binding site completely abolished the oncogenic properties of cIAP1. Further, cIAP1 mediated the clustering of TRAF2, which was sufficient to stimulate tumor growth. Our TRAF2 interactome analysis showed that cIAP1 was critical for TRAF2 to bind to its protein partners. Thus, cIAP1 and TRAF2 would be two essential subunits of a signaling complex promoting a pro-tumoral signal. cIAP1/TRAF2 promoted the activation of the canonical NF-κB and ERK1/2 signaling pathways. NF-κB-dependent production of IL-6 triggered the activation of the JAK/STAT3 axis in an autocrine manner. Inhibition or downregulation of STAT3 specifically compromised the growth of cIAP1-restored MEFs but not that of MEFs expressing a cIAP1-mutant and treating mice with the STAT3 inhibitor niclosamide completely abrogated cIAP1/TRAF2-mediated tumor growth. Altogether, we demonstrate that cIAP1/TRAF2 binding is essential to promote tumor growth via the activation of the JAK/STAT3 signaling pathway.

Introduction

Cellular Inhibitors of apoptosis 1 and 2 (cIAP1/2) and tumor necrosis factor-associated factors 2 (TRAF2) were purified together in 1995 by Rothe *et al.* in a pull-down experiment aiming to identify cytoplasmic components of the tumor necrosis factor receptor-2 (TNFR2) complex (1). cIAP1/2 are RING containing-E3-ubiquitine ligases belonging to the IAP (Inhibitor of apoptosis) family (2). They catalyze the conjugation of ubiquitin chains of different topologies including K6-, K11-, K27-, K48- and K63-linked chains resulting in modification of the stability, activity or interaction network of protein substrates. Their ubiquitination substrates are specifically recruited thanks to the presence of three conserved protein-protein interacting domains named BIRs (Baculoviral IAP repeats) at the N-terminal extremity. More than thirty substrates have been identified so far (3). They comprise cell death regulators such as the IAP antagonist Smac, cell signaling intermediates including receptor-interacting kinases (RIPs), NF-κB-inducing kinase (NIK) and raf proto-oncogene serine/threonine protein kinase (Raf1), regulators of cellular architecture such as some GTPases from the Rho family and transcription factors including E2F1, the Interferon Regulatory Factor 1 (IRF1) and the C/EBP homologous protein (CHOP) (for a review, see(3)). Thus, cIAPs have been involved in the regulation of inflammation, cell differentiation, cell death, cell proliferation and cell migration. cIAP1 is more stronger expressed that cIAP2 in most tissues, except in bone marrow and lymphoid tissues in which cIAP2 is predominant (4). Consistent with its functions in promoting cell survival and proliferation, oncogenic properties of cIAP1 have been demonstrated in several mouse models (5-7).

As cIAP1, TRAF2 is a RING-containing protein. However, its E3-ligase activity seems relatively weak (8, 9). It is considered as a molecular adaptor bridging signaling molecules to receptors (10). It can directly or indirectly bind certain members of TNFR including TNFR1, TNFR2, CD30, CD40 and B-cell activating factor (BAFF-R), toll-like receptor-4 (TLR4), some nucleotide binding-oligomerization domain (NOD)-like receptors (NLRs), retinoic acid-inducible gene I (RIG-1)-like receptors (RLRs) and some cytokine receptors (10). TRAF2 serves as an intermediate for the recruitment of cIAPs into receptor-associated complexes. However, the cIAP1-TRAF2 complex has also been observed in the cytoplasm as well as in the nucleus, independently of receptor engagement (8, 11-14).

Here, by using HRas-V12-transformed mouse embryonic fibroblast (MEF) model, we demonstrated that TRAF2 binding was required for cIAP1 pro-tumoral activity. cIAP1 induced the clustering of TRAF2, which was sufficient to engage pro-tumoral signaling pathways independently of receptor engagement. A novel function for cIAP1 is therefore identified that appears essential for TRAF2 to associate with its protein partners. As expected, cIAP1/TRAF2 complex promoted the activation of the canonical NF-κB signaling pathway. Among mitogen-activated protein kinase (MAPK) signaling pathways, it stimulated ERK1/2 whereas it inhibited p38 and did not affect JNK pathway. cIAP1/TRAF2 promotes NF-κB dependent production of IL-6 that activates JAK2/STAT3 signaling pathway in an autocrine manner. Finally, we demonstrated for the first time that STAT3 activation was critical for the tumor-promoting activity of cIAP1/TRAF2.

Results

1. Binding to TRAF2 is critical for the oncogenic activity of cIAP1.

We generated a cIAP1-deficient tumor model by transforming immortalized wt, *cIap1*$^{-/-}$ (SKO) or *cIap1*$^{-/-}$*/cIap2*$^{-/-}$ (DKO) mouse embryonic fibroblasts (MEFs) (from J. Silke & D. Vaux's laboratories) by the HRas-V12 oncogene (Fig. 1A). Deletion of cIAP1 slowed down tumor growth in a xenograft model (Fig. 1B) and decreased the formation of lung cancer foci when the cells were injected into the tail vein (Fig. 1C). Double deletion of cIAP1 and cIAP2 amplified the phenomena (Fig. 1B and 1C). Rescue experiments demonstrated that restoring cIAP1 in single-knockout (SKO) or double-knockout (DKO) cells (Fig. 1D) significantly enhanced tumor cell growth (Fig 1B & 1E) confirming the oncogenic properties of cIAP1. We next stably expressed cIAP1 mutants unable to bind TRAF2 in Hras-V12-transfomed DKO-MEFs (Fig. 1F). The mutants previously validated (11) are cIAP1$^{\Delta BIR1}$ in which the BIR1 has been deleted, and cIAP1^{L47A} mutant in which a point mutation within the BIR1 has been introduced. We checked that these mutants lost their ability to bind TRAF2 (Fig S1A) and conserved their full E3-ligase activity by treating the cells with the smac mimetic GDC-0152, known to stimulate the self-ubiquitination and degradation of cIAP1 (Fig S1B). Deletion of the BIR1 as well as mutation of Leucine 47 were sufficient to completely abolish the oncogenic activity of cIAP1, as demonstrated both in our xenograft model (Fig 1G) and in the experimental metastasis model (Fig 1H). Re-expression of cIAP1 into DKO also increased the number of the colonies formed in soft agar medium and deletion of BIR1 abolished the capacity of cIAP1

to stimulate anchorage-independent cell growth (Fig 1I). By comparison, deletion of BIR2 (ΔBIR2) did not significantly alter the clonogenic properties (Fig 1I) of cIAP1. Of note, the mutant ΔBIR1, devoid of oncogenic properties, was strongly expressed compared to the native full length cIAP1 (Fig 1F, S1B). These results demonstrate that TRAF2 binding is required for cIAP1 to stimulate tumor growth. It is worth noting that we were unable to obtain TRAF2 depleted MEFs (either by guide-RNA genome editing or shRNA), suggesting that the deletion of TRAF2 caused cell death as already reported (15).

2. Clustering of TRAF2 is sufficient to stimulate tumor growth

An immunofluorescence analysis demonstrated the presence of cytoplasmic TRAF2 clusters in DKO-cIAP1 but not in DKO-cIAP1$^{\Delta BIR1}$ (Fig 2A). Whereas these clusters did not colocalize with markers of calveola (calveolin-1), golgi apparatus (GM130) or lysosomes (LAMP-1), they colocalized with the endoplasmic reticulum marker PDI (Fig 2B). Structural analyzes demonstrated that the BIR1 of cIAPs can bind a TRAF1/2 trimer (16, 17). We hypothesized that cIAP1 could trigger the oligomerization of TRAF2 required for partner binding and the activation of downstream signaling pathways (18). We forced the trimerization of TRAF2 by expressing isolated BIR1 (iBIR1) in DKO-MEFs using a retroviral infection (Fig 2C). As expected, we observed the clustering of TRAF2 in iBIR1-expressing cells (Fig 2A). The expression of iBIR1 increased the clonogenic growth of cells, forming large and dense colonies (Fig 2D) and was as efficient as cIAP1 to stimulate the tumor growth in mice (Fig 2E). Expression of iBIR1 in wt MEFs also stimulated tumor growth (Fig S2A), although the presence of iBIR1 strongly sensitized cells to TNFα-induced cell death (Fig S2B) as a result of a competitive inhibition of cIAP1-TRAF2 association (Fig S2C). These results suggest that TRAF2 clustering is sufficient to engage pro-tumoral signaling pathways, independently of TNFR stimulation.

3. cIAP1 is critical for TRAF2 interactome.

We then investigated the influence of cIAP1 on TRAF2 protein-interacting network. The TRAF2 interactome was analyzed in cell treated with the smac mimetics GDC0152 that completely depleted cIAP1 whereas it weakly enhanced cIAP2 and XIAP and did not affect TRAF2 protein levels (Fig 3A). TRAF2 partners were identified by performing immunoprecipitation (Fig S3A) followed by mass spectrometry analysis (Table S1). The data were analyzed using the functional enrichment analysis tool (FunRich) and the UniProt database. We detected 419 to 797 hits in the untreated cells (Fig 3B). As expected, we found TRAF1 and cIAP1 (BIRC2), which was the only IAP detected in the screen (Fig 3C).

In accordance with its role as a signaling adaptor, we observed an enrichment of TRAF2 partners in the membrane, protein-containing complex and membrane raft compartments (Fig 3D). However, TRAF2 partners were also enriched in the cytoplasm, cytosol and nucleus (Fig 3D, S3B). Concerning biological processes, as expected, TRAF2 partners were enriched among proteins involved in TNF-mediated, NF-κB and MAPK-signaling pathways, apoptosis regulation, proteins ubiquitination and regulation of protein turn-over (protein stabilization and ubiquitin/proteasome system) (Fig 3E, S4). Interestingly, TRAF2 partners were also significantly enriched among proteins involved in epithelial cell differentiation-related pathways (Fig 3E, S4). Use of the FunRich database confirmed a strong enrichment of TRAF2 partners in the ErbB-mediated signaling network, compared to that observed in the TNFR-signaling pathway (Fig S5). Moreover, TRAF2 partners were enriched in cdc42-associated signaling pathways but not in RhoA or Rac1-related signaling events (Fig 3C, S5), which is consistent with our previous work showing that the cytoplasmic cIAP1/TRAF2 complex controls the activation cycle of cdc42 RhoGTPase in unstimulated fibroblasts (11).

cIAP1 depletion drastically decreased (about 70%) the number of hits (Fig 3B, 3F). However, it did not affect the binding of TRAF2 to TRAF1 (Fig 3C) and it did not significantly modify the distribution of TRAF2 partners in the different subcellular compartments, biological processes or signaling pathways (Fig 3D, 3E, S3B, S4, S5). Nevertheless, we observed a trend towards increased TRAF2 partners in negative regulation of apoptosis and protein stabilization pathways (Fig 3E & S4). Thus, cIAP1 appears critical for the binding of TRAF2 to its protein partners.

4. cIAP1/TRAF2 induces the activation of NF-κB and ERK1/2 signaling pathways in H-Ras-V12 transformed MEFs.

We analyzed the signaling pathways activated in HRas-V12-transformed MEFs. As expected, cIAP1-expressing MEFs displays a downregulation of IκB-α (Fig 4A) that characterizes the activation of the canonical NF-κB signaling pathway. This marker was not observed in the mutant cIAP1-expressing cells (Fig 4A). Accordingly, an RT-PCR array showed a general upregulation of NF-κB-target genes in wt cIAP1-expressing MEFs compared to cIAP1$^{\Delta BIR1}$-expressing cells (Fig 4B). On the other hand, the p52 NF-κB active-subunit that is mainly expressed in the nuclei-enriched fraction in DKO cells was found in the cytoplasm in cIAP1-expressing MEFs and even more in cIAP1$^{\Delta BIR1}$-expressing MEFs demonstrating that cIAP1 or its mutant inhibited the non-canonical NF-κB activating pathway (Fig 4C). Among MAPK signaling pathways, expression of cIAP1 but not cIAP1 mutants simulated ERK signaling characterized by ERK1/2 phosphorylation, decreased phosphorylation of p38 and did not affect the c-Jun N-terminal kinase (JNK) signaling

pathway (Fig 4A). Of note, the expression of cIAP1 or its ΔBIR1 mutant did not significantly modify the expression level of TRAF2 and RIP1 (Fig 4A).

5. cIAP1/TRAF2 promotes NF-κB-dependent production of IL-6 leading to an activation of JAK/STAT3 signaling pathway in an autocrine manner.

We observed the activation of JAK2 and STAT3 characterized by their phosphorylation at Y1008 and Y705 residue respectively in cIAP1-expressing MEFs but not in cells expressing cIAP1 mutants (Fig 5A & B). Silencing of TRAF2 decreased cIAP1-mediated STAT3 phosphorylation, confirming the importance of TRAF2 in this process (Fig 5C). We then analyzed the contribution of NF-κB and ERK signaling pathway in STAT3 activation. Inhibition of the NF-κB signaling pathway by Bay-11-7082 prevented STAT3 phosphorylation while inhibition of the MEK/ERK axis by trametinib did not modify it (Fig 5D), demonstrating a NF-κB-dependent activation of STAT3 pathway. Conversely, the STAT3 inhibitor niclosamide did not modify ERK and weakly decreased IκB-α phosphorylation (Fig 5D). Trametinib did not interfere with IκB-α phosphorylation and Bay-11-7082 did not modify ERK phosphorylation (Fig 5D), showing that the 2 pathways were activated independently. JAK2/STAT3 signaling axis can be activated by stimulation of cytokine- or growth factor receptors such as IL-6R or EGFR. Consistent with the activation of NF-κB, cIAP1 expression induced upregulation of the NF-κB target gene *IL-6* which is inhibited by the NF-κB inhibitor Bay-11-7082 but not by the MEK inhibitor Trametinib (Fig 5E). In contrast, the expression of cIAP1$^{\Delta BIR1}$ was not able to stimulate *IL-6* expression (Fig 5E). Inhibition of IL-6 by an anti-IL-6 neutralizing antibody completely blocked STAT3 phosphorylation in cIAP1-restored MEFs (Fig 5F). Altogether, these results demonstrated that the expression of cIAP1 stimulated the NF-κB-dependent production of IL-6 that induced an autocrine activation of the JAK2/STAT3 signaling pathway. By analyzing available cancer genome atlas (TCGA) dataset of the national cancer institute (NIH) using the gene expression profiling interactive analysis software (GEPIA)(19), we observed a significant correlation between the cIAP1-encoding *BIRC2* and *IL6* gene expression in lung adenocarcima (LUAD), breast invasive carcinoma (BRCA) and thyroid carcinoma (THCA) (Fig 5G). In contrast, no correlation between *TNF* and *BIRC2* expression was detected (Fig S6). We then investigated the role of cIAP1 and TRAF2 in JAK/STAT3 signaling in the lung adenocarcinoma cell line A549 (Fig 5H & I). Silencing of cIAP1 or TRAF2 inhibited basal JAK2 and STAT3 phosphorylation (Fig 5H). Similarly, depletion of cIAP1 by GDC-0152 inhibited JAK2 and STAT3 phosphorylation in a dose-dependent manner (Fig 5I).

The JAK/STAT3 signaling pathway is involved in cIAP1-mediated tumor growth.

We then evaluated the contribution of STAT3 and MEK/ERK signaling pathways in cIAP1/TRAF2 mediated-tumor growth using the STAT3 inhibitor niclosamide and the MEK inhibitor trametinib. Niclosamide or trametinib were daily injected intraperitoneally when the tumors reached a volume of approximatively 100 mm^3. Niclosamide treatment selectively slowed down the growth of DKO-cIAP1 MEFs in mice, neutralizing the growth advantage given by cIAP1 expression, whereas it did not modify the growth of $cIAP1^{\Delta BIR1}$ expressing MEFs (Fig 6A & B). In contrast, trametinib inhibited the growth of both MEFs expressing cIAP1 and the ΔBIR1 mutant (Fig 6C & D), which is consistent with the role of MEK/ERK signaling pathway in the transforming activity of HRas-V12. We then confirmed the importance of STAT3 in the growth/survival of cIAP1-expressing MEFs in a clonogenic and crystal violet assay (Fig 6E-G). Inhibition of STAT3 by niclosamide abolished the clonogenic advantage of cIAP1-reconstituted MEFs (Fig 6E) and siRNA-mediated-silencing of STAT3 did not affect the survival of DKO but selectively decreased cIAP1-expressing DKO MEFs count (Fig 6G).

Discussion:

TRAF2 serves as an adaptor protein to bring the cIAP1 E3-ubiquitine ligase closer to its substrates. It can also stabilize cIAP1 protein by blocking its autoubiquitination and degradation (20) and, in some situations, it can activate its E3-ubiquitine ligase activity through K63-linked ubiquitination (21). Conversely, cIAP1 can regulate TRAF2 stability by controlling its ubiquitin-proteasome system (UPS)-mediated degradation (14, 22, 23). In the present work, we extend our understanding of cIAP1's hold over TRAF2 by showing that cIAP1 is critical for TRAF2 binding to its protein partners.

The function of TRAF2 as a molecular adaptor allowing the recruitment of signaling molecules into receptor-associated signaling complexes has been well reported. However, there is converging evidences pointing at the existence of a cIAP1-TRAF2 complex in the cytoplasm and nucleus of unstimulated cells. Shu *et al.* demonstrated in 1996 that cIAP1-TRAF2 binding occurs in the cytoplasm and that they are recruited together to TNFR1-associated complex in TNFα-stimulated cells (24). The TRAF2 protein has a mushroom-like shape. The cap is formed by the C-terminal half of the conserved TRAF domain (called TRAF-C) that mediates binding to receptors, and the stem is formed

by the coiled-coiled N-terminal half of the TRAF domain (TRAF-N), the zing fingers and a N-terminal RING domain required for downstream signaling (18, 25). Whereas the mechanisms of interaction of TRAF2 with receptors have been the subject of numerous studies, the binding of TRAF2 with signaling molecules is much less clear. The trimeric form of TRAF2 binds to activated trimeric receptor (26-28). By contrast, a TRAF2 trimer interacts with only one cIAP1 molecule (16, 17). The oligomerization of the amino-terminal half of TRAF2 is also necessary for the recruitment of downstream signaling effectors (18). The oligomerization site is located in the coiled-coiled TRAF-N domain (26). Of interest, cIAP1 binds a motif called CIM (cIAP1/2-interacting motif) found at the N-terminal extremity of the TRAF-N (16). We may hypothesize that cIAP1 primes TRAF2 for its binding to partners, whether receptors or signaling effectors, by maintaining it in a proficient oligomerized form. Accordingly, we show here that a forced oligomerization of TRAF2 induced by expressing the cIAP1-BIR1 domain is sufficient to engage tumor promoting signaling pathways. Our proteomic analysis revealed that, in the presence of cIAP1, TRAF2 could bind proteins found in different subcellular compartments and involved in different cellular processes. The large number of partners found in the screen suggest that many proteins could potentially be substrates of the cIAP1-TRAF2 E3-ubiquitine ligase complex. Among the TRAFs, we found TRAF1, which is known to bind TRAF2 to form a TRAF1:$(TRAF2)_2$ heterotrimer displaying a higher affinity for cIAP2-BIR1 than the TRAF2 homotrimer (17). Interestingly, depletion of cIAP1 did not affect TRAF2-TRAF1 interaction. Since the analysis has been performed in unstimulated cells, we did not detect receptors in the screen. As expected, TRAF2 partners included proteins involved in TNFR-mediated signaling pathways such as NF-kB, MAPK or apoptosis regulation. In accordance with the E3-ubiquitine ligase activity of the cIAP1/TRAF2 complex, we also found an enrichment of TRAF2 partners involved in ubiquitination-related processes. Interestingly, we observed a strong enrichment of TRAF2 partners among proteins of signaling networks of the ErbB receptors which are activators of the STAT3 axis. Although an interaction of TRAF2 with ErbB receptors has never been observed, a role for TRAF2 in EGF-mediated tumor growth has been reported (29).

We demonstrated that TRAF2 is required for the oncogenic activities of cIAP1 in HRas-V12 expressing cells. The expression of cIAP1 appeared altered in a number of human tumor samples and its overexpression has been correlated with advanced progressive disease, aggressiveness and poor prognosis or low response to treatment (for review, see (30)). Its oncogenic properties have been clearly demonstrated in murine models. In 2006, Zender *et al.* demonstrated that the overexpression of cIAP1 facilitated the growth of $p53^{-/-}$, c-myc-expressing hepatocarcinoma cells in

immunodeficient recipient mice. Inversely downregulation of cIAPs in hepatocarcinoma cells that display a recurrent amplification at the chromosome region containing cIAP1, cIAP2 and Yap1-encoding genes (9qA1 amplicon) selectively slowed down tumor growth (5). Similarly, Ma *et al.* showed that the down-regulation of cIAP1 or cIAP2 selectively affected the growth rate of 9A1 amplicon-harboring, $p53^{-/-}$ osteosarcoma transplanted into nude mice (6). In 2010, Cheng *et al.* demonstrated a high level of expression of cIAP1 and cIAP2 in mammary carcinoma and that the silencing of cIAP1 and/or cIAP2 resulted in decreased tumor growth in an orthotopic breast transplantation model (7). The molecular mechanisms driving these oncogenic activities have not been clearly determined and they probably depend on the oncogenic contexts. The various signaling pathways controlled by cIAPs may account for their tumorigenic functions. The ability of cIAP1 to regulate NF-κBs, a major pro-survival, oncogenic signaling pathway is undeniably of importance in its transforming potential (13, 31, 32). The c-myc repressor Mad1 is an ubiquitination target of cIAP1(33, 34). Thus, the oncogenesis-promoting activity of c-myc can be amplified by cIAP1-mediated downregulation of Mad1. In the present work, we highlighted the importance of the interaction cIAP1 with its protein partner TRAF2 in HRas-V12-driven tumorigenesis. Indeed, preventing the interaction with TRAF2 by deletion or mutation of the BIR1 domain completely abolished the oncogenic potential of cIAP1.

The role of cIAP1-TRAF2 in regulating signaling pathways has been extensively analyzed in the context of stimulation of receptors from the TNFR, IL-R or PRR families (recently reviewed in a special issue of Frontiers in Immunology (35)). Although we cannot rule out that some membrane receptors could be activated by tumor- or host-produced soluble factors in an autocrine or paracrine manner, the oligomerization of TRAF2 by cIAP1 or isolated cIAP1-BIR1 seems sufficient to stimulate tumor-promoting signaling pathways, independently of the stimulation of receptors. Accordingly, Baud *et al.* demonstrated that the overexpression of TRAF2 or oligomerization of its amino-terminal domains was sufficient to activate downstream signaling pathways (18). TRAF2 can directly bind, via its N-terminal half that includes the zing fingers and a N-terminal RING domain, several MAP3Ks including the mixed-lineage protein kinase 3 (MLK3) (36, 37) and ASK1 (38, 39) that drive the activation of SAPK/JNK and p38-MAPK axes, and MEKK1 that induces the activation of downstream SAPK/JNK and NF-κB (18, 40). The ubiquitin chains conjugated by the cIAP1/TRAF2 E3-ubiquitin ligase complex (to RIP1 or via a self-ubiquitination process) are scaffolds for the recruitment of TAK1 and IKKγ that lead to MAPK and canonical NF-kB activation (41). Moreover, cIAP1 can control the activation of the RAF-MEK-ERK1/2 cascade by ubiquitinating cRAF (42). In the present work, we observed that the tumor-promoting activity of cIAP1/TRAF2 was associated with an activation of the canonical NF-κB and ERK1/2 whereas JNK

and p38MAPK signaling pathways were unaffected or inhibited. More investigations will be required to determine the downstream effectors. Expressing cIAP1 induced a decreased in the non-canonical activation of NF-κB, in accordance with its capacity to target NIK to UPS-mediated degradation (21, 43). The deletion of the BIR1 domain amplified the phenomena. Lee *et al*. identified an IBM (IAP-binding motif) at the N-terminus of NIK protein sequence (43). The NIK-IBM is recognized by the BIR2 domain of cIAP1 and constitutes a substrate recognition signal for cIAP1-mediated ubiquitination and degradation (43). We may hypothesize that the deletion of BIR1 could improve the accessibility to the BIR2 domain leading to an enhanced recruitment and degradation of NIK.

Last, we demonstrate here that cIAP1/TRAF2 promotes the activation of the JAK/STAT3 axis. The activation of this signaling pathway results from an NF-κB-dependent production of IL-6 and autocrine activation of IL-6 signaling pathway. The presence of IL-6 in the tumor environment and hyperactivation of the JAK/STAT3 signaling pathway in cancer cells have been found in different kind of tumors (44). The analysis of TCGA dataset revealed a positive correlation between cIAP1-encoding gene and *IL-6* in lung, breast and thyroid carcinoma. The smac mimetic GDC-0152 as well as downregulation of cIAP1 or TRAF2 were able to decrease the activation of STAT3 in A549 lung carcinoma cells suggesting that cIAP1/TRAF2 could account for the activation of STAT3 in these cells. Interestingly, we show here that inhibition of STAT3 by niclosamide completely abrogated the tumor growth advantage given by expressing cIAP1 demonstrating that the activation of the STAT3 axis is required for the tumor-promoting activity of cIAP1.

The current model supports that TRAF2 acts solely as an adaptor protein recruiting the cIAP1/cIAP2 E3-ligase in the receptor-associated complex. Our work demonstrates that (i) oligomerisation of TRAF2 is sufficient to stimulate pro-tumoral signaling pathways, (ii) TRAF2 is a critical regulator of the oncogenic activity of cIAP1 and (iii) cIAP1 is essential for TRAF2' capacity to bind signaling molecules, independently of receptor activation. The cIAP1-encoding *BIRC2* gene as well as *TRAF2* are found recurrently amplified in human epithelial cancers (30, 45). IAPs constitute promising target for anticancer therapy and a number of IAP antagonists have been developed and are currently under clinical investigation (30). Most of them are Smac mimetics that block the anti-apoptotic activity of XIAP and induce the degradation of cIAP1 and, in some cases, other members of the IAP family. Considering our results, it could be interesting to develop molecules able to inhibit the oligomerisation of TRAF2 or the cIAP1-TRAF2 interaction.

Materials and methods:

Cell culture and treatments:

SV40 immortalized wt, cIAP1$^{-/-}$ (single Knock out, SKO) and cIAP1$^{-/-}$/cIAP2$^{-/-}$ (double KO, DKO) mouse embryonic fibroblasts (MEFs) (J. Silke & D. Vaux, Melbourne, Australia), A549 human lung carcinoma cell line, HeLa cervical carcinoma cell line and Phoenix-Eco 293T cells (Invitrogen, Carlsbad, USA) were cultured in DMEM (Dulbecco's modified Eagle's medium, Dominique Dutscher, Brumath, France) high glucose medium supplemented with 10% fetal bovine serum (Dominique Dutscher) at 37°C, 5% CO_2 environment. MEFs were transformed by HRas-V12 as previously described (11). MEFs were treated with 1-2µM niclosamide, 2µM Bay-11-7082, 2µM Trametinib (Euromedex, Souffelweyersheim, France) or 100 ng/mL anti-IL-6 neutralizing antibody (Invivogen, San Diego, USA). GDC0152 (Euromedex) was used at 1 to 5µM.

Plasmid constructs, siRNAs, cell transfection and viral transduction:

Plasmids used were: pMSCV-control, pMSCV-cIAP1, pMSCV-cIAP1ΔBIR1, pMSCV-cIAP1ΔBIR2, pMSCV-cIAP1-L47A, pMSCV-iBIR1 (cIAP1). Cells were transfected using Jet PEI transfection reagent (Polyplus transfection, Ozyme, France) for plasmids or Lipofectamine® RNAimax (Thermofisher Scientific, Waltham, USA) for siRNAs against human cIAP1 (#SI02654442), human TRAF2 (#SI00129619), mouse TRAF2 (#SI01454544) or human STAT3 (#1: SI01435294 and #2: SI01435287) from Qiagen (Hilden, Germany).Phoenix-Eco 293T cells used for viral production were transfected using Jet PEI. For the infection of MEFs, retrovirus-containing supernatant was supplemented with 1µg/mL of polybrene (Sigma-Aldrich, St-Louis, USA). Cells were selected with 2.8µg/mL of puromycine.

In vivo experiments:

Nude (NMRI-Foxn1nu/Foxn1nu) mice (Charles River Laboratories, Saint-Germain-Nuelles, France) (female between 6 and 8 weeks old) were housed in pathogen free conditions in zootechny center (certification n°C21 464 04 EA). All studies were approved by the Ethics Committee for Animal Welfare of the University of Burgundy and the French Ministry of Higher Education and Research (APAFIS#5438-201611301622214). For subcutaneous tumors, mice were

randomized and inoculated subcutaneously with 500 000 or 750 000 HRas-V12-transformed MEFs. When the tumors reached 100mm^3, mice were allocated into experimental groups so that the mean +/- SD was equivalent in each of the groups and daily treated intraperitoneally with niclosamide (30 mg/Kg), trametinib (1mg/kg) or vehicle. Tumor volume was measured with calipers and calculated as proposed by Laval University (Québec, Canada): (4/3)*3.14159*(length/2)*(width/2)^2. For artificial metastasis model, HRas-V12-transformed MEFs were injected into the tail vein (10^6) in a volume of 100µL. Mice were sacrificed 36 days after intravenous injection of the cells. Lung nodes were counted by macroscopic analysis. The experiments were performed at least twice n=6-10 per group. Statistical analyses were performed using the Mann Whitney test.

Cell extracts, subcellular fractionation, immunoprecipitation and Western Blot:

Cells were washed in cold 1X DPBS (Dulbecco's Phosphate Buffer Saline, Dominique Dustcher, Brumath, France) and lysed in RIPA buffer (50mM Tris-HCl pH 8,0 ; 150mM NaCl ; 1% NP-40 ; 0.5% Sodium deoxycholate, 0.1% SDS, 1mM sodium orthovanadate, 1mM PMSF) supplemented with a proteases inhibitor cocktail (PIC, Sigma-Aldrich, St-Louis, USA) and phosphatase inhibitor cocktail PhosSTOP™ (Merck, Darmstadt, Germany). The subcellular fractionation was performed by lysing cells in 10mM Hepes, 10mM KCl, 0.1mM EDTA, 0.1mM EGTA, 1mM DTT (DiThioThreitol) for 15 minutes on ice. NP-40 (0.6% final) was added to the lysate which then subjected to centrifugation at 1200g for 5 minutes at 4°C. The supernatant containing the cytoplasmic fraction was collected. The pellet was lysed in 100µL of 50mM Tris-HCL pH8.0, 150mM NaCl, 1%NP-40 for 15 minutes on ice. The solution was centrifuged at 16000g for 15 minutes at 4°C and the supernatant containing the nuclear fraction is collected. Proteins were quantified using the Precision Red Advanced Protein Assay ADV02 kit (Cytoskeleton, Denver, USA).

For Immunoprecipitation, cells were lysed in IP buffer (50mM Tris HCL ph7.4, 150mM NaCl, 20mM EDTA, 0.5% NP-40, Protease inhibitor cocktail 1X). Cell lysates were incubated with anti-TRAF2 (#ab126758, Abcam, Cambridge, UK) antibodies overnight at 4°C. The lysates were then incubated 2 hours with G Sepharose beads (Merk-Millipore, Fontenay-sous-bois, France). Proteins were eluted by heating the mix to 95°C for 10 minutes in 1X Laemmli buffer (Tris-HCl 150 mM pH 6,8 ; β-mercaptoethanol 15 %; SDS 6 %; glycerol 30 %; Bromophenol blue). For the Western blot analysis, proteins were separated on SDS-PAGE and electro-transferred onto polyvinylidene difluoride or nitrocellulose

membranes (GE Healthcare, Dominique Dutscher, Brumath, France). Blots were probed with the following antibodies: anti-cIAP1 (#AF8181, R&D systems, Minneapolis, USA) and anti-pan-cIAPs (#MAB3400, R&D systems, Minneapolis, USA), anti-TRAF2 (#ADI-AAP-422, Enzo Life Sciences, Villeurbanne, France), anti-RIP1 (#610459, BD biosciences, USA), anti-IκBα (#4812S), anti-p-IκBα (S32, #2859S), anti-ERK1/2 (#4695T), anti-p-ERK1/2 (Y202/204, #4370T), anti-JNK (#9252T), anti-p-JNK (T183/Y185, #81E11), anti-p38 (#D13E1), anti-p-p38 (T180/Y182, #D3F9), anti-STAT3 (#D3Z2G), anti-p-STAT3 (Y705, #D3A7), anti-JAK2 (#D2E12) and anti-p-JAK2 (Y1008, #D4A8) and anti-p100/p52 NFκB (#4882) from Cell signaling technologies (Danvers, USA), anti-HSC70 (sc-7298, Santa Cruz Biotechnology Inc, Dallas, USA) and anti-β-actin (#MA1-140 Invitrogen, Waltham, USA), Anti-XIAP (AF8221, R&D systems) and anti-Ras (sc-520, Santa cruz Technology Inc). Detection was performed using peroxidase-conjugated secondary antibodies and chemiluminescence detection kit (Clarity™ or Clarity Max™ western ECL substrate, Bio-Rad, Marnes-la-Coquette, France). GST-pull down assays were performed as previously described (11).

Immunofluorescence: Cells were washed in cold 1X DPBS and fixed for 10 min in 4% paraformaldehyde/PBS, permeabilized using 0.1% triton X-100 (10 minutes) and saturated for 20 minutes in PBS with 1% bovine serum albumin and 1% of fetal bovine serum. Samples were incubated overnight at 4°C in PBS-1%BSA with primary antibodies anti-GM130 (#610823, BD Bioscience), anti-Caveolin-1 (#MA3-600, Invitrogen), anti-LAMP-1 (#ab25245, Abcam) or anti-PDI (#3501, Cell Signaling), washed and incubated with secondary antibodies goat anti-rat Alexa568, goat anti-mouse alexa568 or donkey anti-rabbit Alesa568 (Invitrogen) diluted in PBS-1%BSA at room temperature for 1h. Samples were then incubated with Alexa488 labeled anti-TRAF2 antibody (Abcam ab198971) diluted in PBS-1%BSA overnight at 4°C. Samples were washed for 10 minutes three times, then mounted using ProLong™ Gold Antifade Mountant with DAPI (Thermofisher Scientific, Waltham, USA). Sample images were acquired using an Axio Imager 2 using an Apotome.2 module, HXP 120C illumination, Axiocam MRm using a 64x 1.4NA objective.

RNA extraction and RT-qPCR: Total RNA of MEF DKO expressing or not cIAP1 or its mutants were extracted with Trizol reagent (TRizol Reagent ®, Invitrogen) according to manufacturer's protocol. Tumors from in vivo experiments were crushed in 1mL of Trizol to extract their RNA. cDNA was produced from 1µg of RNA with iScript cDNA synthesis kit

(Biorad, Hercules, USA). Quantitative real-time PCR was performed with ViiA 7 Real-Time PCR System (Applied Biosystem, ThermoFisher Scientific, Waltham, USA) using Master Mix Applied Biosystems™ PowerUp™ SYBR™ Green (Thermofisher Scientific, Waltham, USA) and the following primers: β-Actin Forward : CGG-TTC-CGAT-GCC-CTG-AGG-CTC-TT, Reverse : CGT-CAC-ACTTCA-TGA-TGG-AAT-TGA ; IL-6 (Interleukine 6) Forward : TGA-TGC-ACT-TGC-AGA-AAA-CA, Reverse : ACC-AGA-GGA-AAT-TTT-CAA-TAG-GC.

For the qPCR microarray, cDNA from MEF DKO-cIAP1 and MEF DKO-cIAP1ΔBIR1 RNA were analyzed using Qiagen NF-κB Signaling Pathway RT^2 Profiler PCR Array according to manufacturer's protocol.

Clonogenic assay: Five thousand MEFs were seeded in soft-agar medium for 3 weeks at 37°C in a 5% CO_2 atmosphere. They were treated with 1-2 µM Niclosamide before plating. Colony number and size were analyzed under microscope (Zeiss, Oberkochen, Germany), and images were taken using AxioVision software.

Cristal violet assay: One hundred thousand were plated in 6-wells plate. Seventy-two hours later, cells were fixed and stained with a 0.5% Crystal violet in methanol solution. Crystal violet was eluted with 37% acetic acid, and the OD at 620nm was measured with a UVM 340 plate reader (Biochrom, Cambourne, UK).

Mass-spectrometry: A549 cells were treated or not with 5µM of GDC-0152 for 6 hours. TRAF2 was immunoprecipitated and eluted. ESI-TRAP mass spectrometry was performed by the CLIPP platform as described previously (46) Data were analyzed with FunRich software, version 3.1.3 (Functional enrichment analysis tool)(47), using the human Uniprot or FunRich database.

Statistical analysis: the correlation analysis of the cIAP1, IL-6 and TNF-α expression in tumor samples was done using the publicly available TCGA dataset using gene expression profiling interactive analysis (GEPIA), using the Pearson Correlation Coefficient. The non-parametric Mann–Whitney test was used for the analysis of tumor growth in animals and RT-qPCR and Wilcoxon test for clonogenic and western blot analyses.

Acknowledgements. We thank Pauline Maes from the CLIPP proteomic platform, University of Burgundy, Philippe Hammann from the Strasbourg proteomic platform, IBMC, Valérie Saint-Gorgio from zootechny center, University of Burgundy and Romain Aucagne from the Crigen platform, University of Burgundy. This work was supported by grants

from the 'Comités de Côte d'Or et de l'Yonne' of the 'Ligue Contre le Cancer' (LD), La Ligue Nationale contre le Cancer (CG's team), the European Union and the 'Conseil Régional de Bourgogne', a French Government grant managed by the French National Research Agency under the program 'Investissements d'Avenir' with reference ANR-11-LABX-0021, and fellowships from the 'Ministère de l'Enseignement Supérieur et de la Recherche' of France (to BD, AZ, JB and JA), the 'Fondation ARC pour la Recherche sur le Cancer' (to BD). We thank the FEDER for their financial support.

Author contributions. BD and AZ performed most of the experiments and analyzed the data. JB initiated the project, established the tumor model and performed some *in vivo* experiments. SC performed immunofluorescence analysis. JA, PB and FC helped in performing western blots, clonogenicity assays and *in vivo* experiments. CR and CP brought expertise in *in vivo* model and performed IV injection. CG provided scientific expertise and corrected the paper and LD conceived and supervised the project, conducted the GEPIA analysis, analyzed the data and interpreted the results, wrote the paper with input from all authors.

References

1. Rothe M, Pan MG, Henzel WJ, Ayres TM, Goeddel DV. The TNFR2-TRAF signaling complex contains two novel proteins related to baculoviral inhibitor of apoptosis proteins. Cell. 1995;83(7):1243-52.
2. Hrdinka M, Yabal M. Inhibitor of apoptosis proteins in human health and disease. Genes Immun. 2019;20(8):641-50.
3. Dumetier B, Zadoroznyj A, Dubrez L. IAP-Mediated Protein Ubiquitination in Regulating Cell Signaling. Cells. 2020;9(5).
4. Zadoroznyj A, Dubrez L. Cytoplasmic and Nuclear Functions of cIAP1. Biomolecules. 2022;12(2).
5. Zender L, Spector MS, Xue W, Flemming P, Cordon-Cardo C, Silke J, et al. Identification and validation of oncogenes in liver cancer using an integrative oncogenomic approach. Cell. 2006;125(7):1253-67.
6. Ma O, Cai WW, Zender L, Dayaram T, Shen J, Herron AJ, et al. MMP13, Birc2 (cIAP1), and Birc3 (cIAP2), amplified on chromosome 9, collaborate with p53 deficiency in mouse osteosarcoma progression. Cancer Res. 2009;69(6):2559-67.
7. Cheng L, Zhou Z, Flesken-Nikitin A, Toshkov IA, Wang W, Camps J, et al. Rb inactivation accelerates neoplastic growth and substitutes for recurrent amplification of cIAP1, cIAP2 and Yap1 in sporadic mammary carcinoma associated with p53 deficiency. Oncogene. 2010;29(42):5700-11.
8. Jin J, Xiao Y, Hu H, Zou Q, Li Y, Gao Y, et al. Proinflammatory TLR signalling is regulated by a TRAF2-dependent proteolysis mechanism in macrophages. Nat Commun. 2015;6:5930.
9. Yin Q, Lamothe B, Darnay BG, Wu H. Structural basis for the lack of E2 interaction in the RING domain of TRAF2. Biochemistry. 2009;48(44):10558-67.
10. Dhillon B, Aleithan F, Abdul-Sater Z, Abdul-Sater AA. The Evolving Role of TRAFs in Mediating Inflammatory Responses. Front Immunol. 2019;10:104.
11. Marivin A, Berthelet J, Cartier J, Paul C, Gemble S, Morizot A, et al. cIAP1 regulates TNF-mediated cdc42 activation and filopodia formation. Oncogene. 2014;33(48):5534-45.

12. Vischioni B, Giaccone G, Span SW, Kruyt FA, Rodriguez JA. Nuclear shuttling and TRAF2-mediated retention in the cytoplasm regulate the subcellular localization of cIAP1 and cIAP2. Exp Cell Res. 2004;298(2):535-48.
13. Zhou AY, Shen RR, Kim E, Lock YJ, Xu M, Chen ZJ, et al. IKKepsilon-mediated tumorigenesis requires K63-linked polyubiquitination by a cIAP1/cIAP2/TRAF2 E3 ubiquitin ligase complex. Cell reports. 2013;3(3):724-33.
14. Dupoux A, Cartier J, Cathelin S, Filomenko R, Solary E, Dubrez-Daloz L. cIAP1-dependent TRAF2 degradation regulates the differentiation of monocytes into macrophages and their response to CD40 ligand. Blood. 2009;113(1):175-85.
15. Kreckel J, Anany MA, Siegmund D, Wajant H. TRAF2 Controls Death Receptor-Induced Caspase-8 Processing and Facilitates Proinflammatory Signaling. Front Immunol. 2019;10:2024.
16. Mace PD, Smits C, Vaux DL, Silke J, Day CL. Asymmetric recruitment of cIAPs by TRAF2. J Mol Biol. 2010;400(1):8-15.
17. Zheng C, Kabaleeswaran V, Wang Y, Cheng G, Wu H. Crystal structures of the TRAF2: cIAP2 and the TRAF1: TRAF2: cIAP2 complexes: affinity, specificity, and regulation. Mol Cell. 2010;38(1):101-13.
18. Baud V, Liu ZG, Bennett B, Suzuki N, Xia Y, Karin M. Signaling by proinflammatory cytokines: oligomerization of TRAF2 and TRAF6 is sufficient for JNK and IKK activation and target gene induction via an amino-terminal effector domain. Genes Dev. 1999;13(10):1297-308.
19. Tang Z, Li C, Kang B, Gao G, Zhang Z. GEPIA: a web server for cancer and normal gene expression profiling and interactive analyses. Nucleic Acids Res. 2017;45(W1):W98-W102.
20. Csomos RA, Brady GF, Duckett CS. Enhanced cytoprotective effects of the inhibitor of apoptosis protein cellular IAP1 through stabilization with TRAF2. J Biol Chem. 2009;284(31):20531-9.
21. Vallabhapurapu S, Matsuzawa A, Zhang W, Tseng PH, Keats JJ, Wang H, et al. Nonredundant and complementary functions of TRAF2 and TRAF3 in a ubiquitination cascade that activates NIK-dependent alternative NF-kappaB signaling. Nat Immunol. 2008;9(12):1364-70.
22. Li X, Yang Y, Ashwell JD. TNF-RII and c-IAP1 mediate ubiquitination and degradation of TRAF2. Nature. 2002;416(6878):345-7.
23. Matsuzawa A, Tseng PH, Vallabhapurapu S, Luo JL, Zhang W, Wang H, et al. Essential cytoplasmic translocation of a cytokine receptor-assembled signaling complex. Science. 2008;321(5889):663-8.
24. Shu HB, Takeuchi M, Goeddel DV. The tumor necrosis factor receptor 2 signal transducers TRAF2 and c-IAP1 are components of the tumor necrosis factor receptor 1 signaling complex. Proc Natl Acad Sci U S A. 1996;93(24):13973-8.
25. Borghi A, Verstrepen L, Beyaert R. TRAF2 multitasking in TNF receptor-induced signaling to NF-κB, MAP kinases and cell death. Biochem Pharmacol. 2016;116:1-10.
26. Ceccarelli A, Di Venere A, Nicolai E, De Luca A, Minicozzi V, Rosato N, et al. TNFR-Associated Factor-2 (TRAF2): Not Only a Trimer. Biochemistry. 2015;54(40):6153-61.
27. Ye H, Park YC, Kreishman M, Kieff E, Wu H. The structural basis for the recognition of diverse receptor sequences by TRAF2. Mol Cell. 1999;4(3):321-30.
28. Park HH. Structure of TRAF Family: Current Understanding of Receptor Recognition. Front Immunol. 2018;9:1999.
29. Peng C, Zhu F, Wen W, Yao K, Li S, Zykova T, et al. Tumor necrosis factor receptor-associated factor family protein 2 is a key mediator of the epidermal growth factor-induced ribosomal S6 kinase 2/cAMP-responsive element-binding protein/Fos protein signaling pathway. J Biol Chem. 2012;287(31):25881-92.
30. Dubrez L, Berthelet J, Glorian V. IAP proteins as targets for drug development in oncology. OncoTargets and therapy. 2013;9:1285-304.
31. Park MH, Hong JT. Roles of NF-κB in Cancer and Inflammatory Diseases and Their Therapeutic Approaches. Cells. 2016;5(2).
32. Vu NT, Park MA, Shultz MD, Bulut GB, Ladd AC, Chalfant CE. Caspase-9b Interacts Directly with cIAP1 to Drive Agonist-Independent Activation of NF-κB and Lung Tumorigenesis. Cancer Res. 2016;76(10):2977-89.
33. Xu L, Zhu J, Hu X, Zhu H, Kim HT, LaBaer J, et al. c-IAP1 cooperates with Myc by acting as a ubiquitin ligase for Mad1. Mol Cell. 2007;28(5):914-22.
34. Li H, Fang Y, Niu C, Cao H, Mi T, Zhu H, et al. Inhibition of cIAP1 as a strategy for targeting c-MYC-driven oncogenic activity. Proc Natl Acad Sci U S A. 2018;115(40):E9317-E24.
35. Bishop GA, Abdul-Sater AA, Watts TH. Editorial: TRAF Proteins in Health and Disease. Front Immunol. 2019;10:326.
36. Sondarva G, Kundu CN, Mehrotra S, Mishra R, Rangasamy V, Sathyanarayana P, et al. TRAF2-MLK3 interaction is essential for TNF-alpha-induced MLK3 activation. Cell Res. 2010;20(1):89-98.

37. Korchnak AC, Zhan Y, Aguilar MT, Chadee DN. Cytokine-induced activation of mixed lineage kinase 3 requires TRAF2 and TRAF6. Cell Signal. 2009;21(11):1620-5.
38. Zhao Y, Conze DB, Hanover JA, Ashwell JD. Tumor necrosis factor receptor 2 signaling induces selective c-IAP1-dependent ASK1 ubiquitination and terminates mitogen-activated protein kinase signaling. J Biol Chem. 2007;282(11):7777-82.
39. Nishitoh H, Saitoh M, Mochida Y, Takeda K, Nakano H, Rothe M, et al. ASK1 is essential for JNK/SAPK activation by TRAF2. Mol Cell. 1998;2(3):389-95.
40. Chadee DN, Yuasa T, Kyriakis JM. Direct activation of mitogen-activated protein kinase kinase kinase MEKK1 by the Ste20p homologue GCK and the adapter protein TRAF2. Mol Cell Biol. 2002;22(3):737-49.
41. Annibaldi A, Meier P. Checkpoints in TNF-Induced Cell Death: Implications in Inflammation and Cancer. Trends Mol Med. 2018;24(1):49-65.
42. Dogan T, Harms GS, Hekman M, Karreman C, Oberoi TK, Alnemri ES, et al. X-linked and cellular IAPs modulate the stability of C-RAF kinase and cell motility. Nat Cell Biol. 2008;10(12):1447-55.
43. Zarnegar BJ, Wang Y, Mahoney DJ, Dempsey PW, Cheung HH, He J, et al. Noncanonical NF-kappaB activation requires coordinated assembly of a regulatory complex of the adaptors cIAP1, cIAP2, TRAF2 and TRAF3 and the kinase NIK. Nature immunology. 2008;9(12):1371-8.
44. Johnson DE, O'Keefe RA, Grandis JR. Targeting the IL-6/JAK/STAT3 signalling axis in cancer. Nat Rev Clin Oncol. 2018;15(4):234-48.
45. Zhu S, Jin J, Gokhale S, Lu AM, Shan H, Feng J, et al. Genetic Alterations of TRAF Proteins in Human Cancers. Front Immunol. 2018;9:2111.
46. Didelot C, Lanneau D, Brunet M, Bouchot A, Cartier J, Jacquel A, et al. Interaction of heat-shock protein 90 beta isoform (HSP90 beta) with cellular inhibitor of apoptosis 1 (c-IAP1) is required for cell differentiation. Cell Death Differ. 2008;15(5):859-66.
47. Pathan M, Keerthikumar S, Ang CS, Gangoda L, Quek CY, Williamson NA, et al. FunRich: An open access standalone functional enrichment and interaction network analysis tool. Proteomics. 2015;15(15):2597-601.

Figure legends

Figure 1. TRAF2 binding is critical for the oncogenic activity of cIAP1. Wild type (wt), cIAP1 $^{-/-}$ (SKO) or cIAP1$^{-/-}$/cIAP2$^{-/-}$ (DKO) mouse embryonic fibroblasts (MEFs) were transformed by Hras-V12 oncogene and reconstituted with cIAP1, or cIAP1 mutants cIAP1$^{\Delta BIR1}$ (ΔBIR1), cIAP1^{L47A} (L47A) or cIAP1$^{\Delta BIR2}$ (ΔBIR2). **A, D, F.** Western blot analysis of cIAPs and Ras. HSC70 was used as loading control. **B, E, G.** Cells (500 000) were injected subcutaneously in nude NMRI mice. Tumor size was measured every two days (B), 17 (E) or 3 weeks (G) post-injection. Statistical analyses were performed using the Mann Whitney test. Mean ± SEM (B) or Mean ± SD (E, G), n=10-30. In B, the statistical analyses compared SKO or DKO with cIAP1-expressing SKO or DKO respectively. **C, H.** Cells (10^6) were injected in the caudal vein in nude NMRI mice. The number of lung foci was determined 36 days after intravenous injection. Statistical analyses were performed using the Mann Whitney test. Mean ± SD, n=8-20. **I.** Clonogenic growth of cells in soft agar medium. Statistical analyses were performed using the Wilcoxon test. Mean ± SD, n=3-5.

Figure 2. Forced clustering of TRAF2 stimulated tumor growth, independently of cIAP1. cIAP1, cIAP1$^{\Delta BIR1}$ or the isolated cIAP1-BIR1 domain (iBIR1) were expressed in HRas-V12-transformed DKO MEFs. **A.** Immunofluorescence analysis of TRAF2 in DKO, DKO-cIAP1, DKO-cIAP1$^{\Delta BIR1}$ (ΔBIR1) or DKO-iBIR1. Scale bars: 10µm. **B.** Immunofluorescence analysis of TRAF2 and indicated organelle markers in DKO-cIAP1. Scale bars: 7µm. **C.** Western blot analysis of cIAP1. β-actin was used as loading control. **D.** Colonies formed in soft-agar medium. Scale bars: 100µm. **E.** DKO, DKO-cIAP1 and DKO-iBIR1 MEFs (500 000) were subcutaneously injected into nude mice. Tumor volume 24 days after injection is represented. Statistical analyses comparing the DKO group and cIAP1 or iBIR1-expressing group were performed using the Mann Whitney test. Mean ± SEM, n=12-13.

Figure 3. TRAF2 interactome. A549 cells were incubated for 6 hours with vehicle (NT) or 5µM GDC-0152 (GDC). TRAF2 was immunoprecipitated and its interactome was analyzed by ESI-TRAP mass spectrometry. Analysis was performed using the functional enrichment analysis tool (FunRich) using the FunRich (B, F) or UniProt (D, E) databases. **A.** Western blot analysis of cIAP1, cIAP2, XIAP and TRAF2. HSC70 was used as loading control. **B, F.** Number of partners of TRAF2 in untreated (NT) or GDC-0152-treated cells. Mean ± SD, n=3 (NT) or 2 (GDC-0152). **C.** Peptides identified by mass spectrometry after TRAF2 immunoprecipitation. **D, E.** Enrichment of TRAF2 partners in

subcellular compartments (D) and biological processes (E). Mean ± SD, n=3 (NT) or 2 (GDC-0152). **F.** Venn diagram. One representative experiment is shown.

Figure 4. TRAF2 binding is essential for the activation of the canonical NF-κB and ERK1/2 signaling pathways. A. Western blot analysis of proteins involved in the canonical NF-κB, p38-MAPK, ERK1/2 and JNK signaling pathways. β-actin or HSC70 were used as loading control. **B.** NF-κB target genes were analyzed in MEF DKO-cIAP1 and DKO-cIAP1$^{\Delta BIR1}$ by RT-qPCR array (Qiagen NFkB Signaling Pathway RT2 Profiler PCR Array). **C.** Western blot analysis of the NF-κB p52 subunit in cytoplasmic and nuclear-enriched fractions. XIAP was used as cytoplasmic fraction control and HSC70 as a loading control.

Figure 5. **cIAP1 and TRAF2 are critical for the activation of the JAK/STAT3 signaling pathways. A.** Western blot analysis of the proteins involved in the JAK/STAT3 signaling pathway in MEF DKO expressing cIAP1, cIAP1$^{\Delta BIR1}$ or cIAP1^{L47A}. HSC70 is used as loading control **B.** p-STAT3 was quantified using the Image J software. Mann-Whitney statistical analysis, mean ± SD of 3 independent experiments is shown. **C.** MEFs were transfected with TRAF2-targeting siRNAs. TRAF2 and STAT3 phosphorylation were analyzed by western blot. β-actin was used as loading control. Sc: scramble siRNA. **D.** cIAP1-expressing DKO MEFs (DKO-cIAP1) were treated for 4hrs with 2µM Bay-11-7082, 2µM trametinib or 2µM niclosamide. Western blot analysis of indicated proteins. HSC70 is used as loading control. **E.** RT-qPCR analysis of IL-6 mRNA level in MEFs DKO, DKO-cIAP1 and DKO-cIAP1$^{\Delta BIR1}$ or DKO-cIAP1 treated for 4 hrs with 2µM Bay-11-7082 or 2µM trametinib. Mann Whitney test. Mean ± SD, n=3. **F.** Western blot analysis of the phosphorylation of STAT3 in DKO and DKO-cIAP1 MEFs incubated in the presence of neutralizing anti-IL-6 antibody (100ng/mL) for 24hrs. **G.** Correlative analysis of the expression of *IL6* and cIAP1-encoding *BIRC2* genes in lung adenocarcinoma (LUAD), breast invasive carcinoma (BRCA) and thyroid carcinoma (THCA) using the publicly available TCGA dataset and gene expression profiling interactive analysis (GEPIA) tools. **H, I.** Western blot analysis of the proteins involved in the JAK2/STAT3 signaling pathway in A549 lung carcinoma cells transfected with siRNAs directed against cIAP1 or TRAF2 (H) or treated for 6 hours with the indicated concentration of the smac mimetic GDC-0152 (I). HSC70 was used as loading control.

Figure 6. **STAT3 signaling pathway is required for cIAP1-mediated tumor cell growth.**

A-D. DKO-cIAP1 or DKO cIAP1$^{\Delta BIR}$ MEFs (750 000) were subcutaneously injected into nude mice. When the tumor reached 100 mm^3 (indicated by the narrow), mice were daily treated by intraperitoneal injection of vehicle (NT group) or 30 mg/Kg niclosamide (**A, B**) or 1mg/kg trametinib **(C, D).** Tumor size was measured every two days (**A, C**) or 25-26 days after cell challenge (**B, D**). The results of the statistical analyzes comparing the vehicle with niclosamide or trametinib-treated DKO-cIAP1 mice groups are indicated above the graphs while those comparing vehicle with niclosamide or trametinib-treated DKO cIAP1$^{\Delta BIR}$ are indicated below. Mann Whitney test, mean ± SEM (A,C) or mean ± SD (B,D) , n=12-14. **E.** Clonogenic growth of DKO-cIAP1 and DKO-cIAP1$^{\Delta BIR1}$ MEFs incubated in the presence of vehicle (0) or indicated concentrations of niclosamide. The Wilcoxon test was used for statistical analysis, Mean ± SD, n=3. **F, G.** DKO or cIAP1-expressing DKO MEFs were transfected with control (Ctl) or STAT3-directed siRNAs (#1, #2). Western blot analysis of STAT3 (**F**) and cell count 72hrs after transfection (**G**). The Wilcoxon test was used for statistical analysis, Mean ± SD, n=3.

FIGURE 1

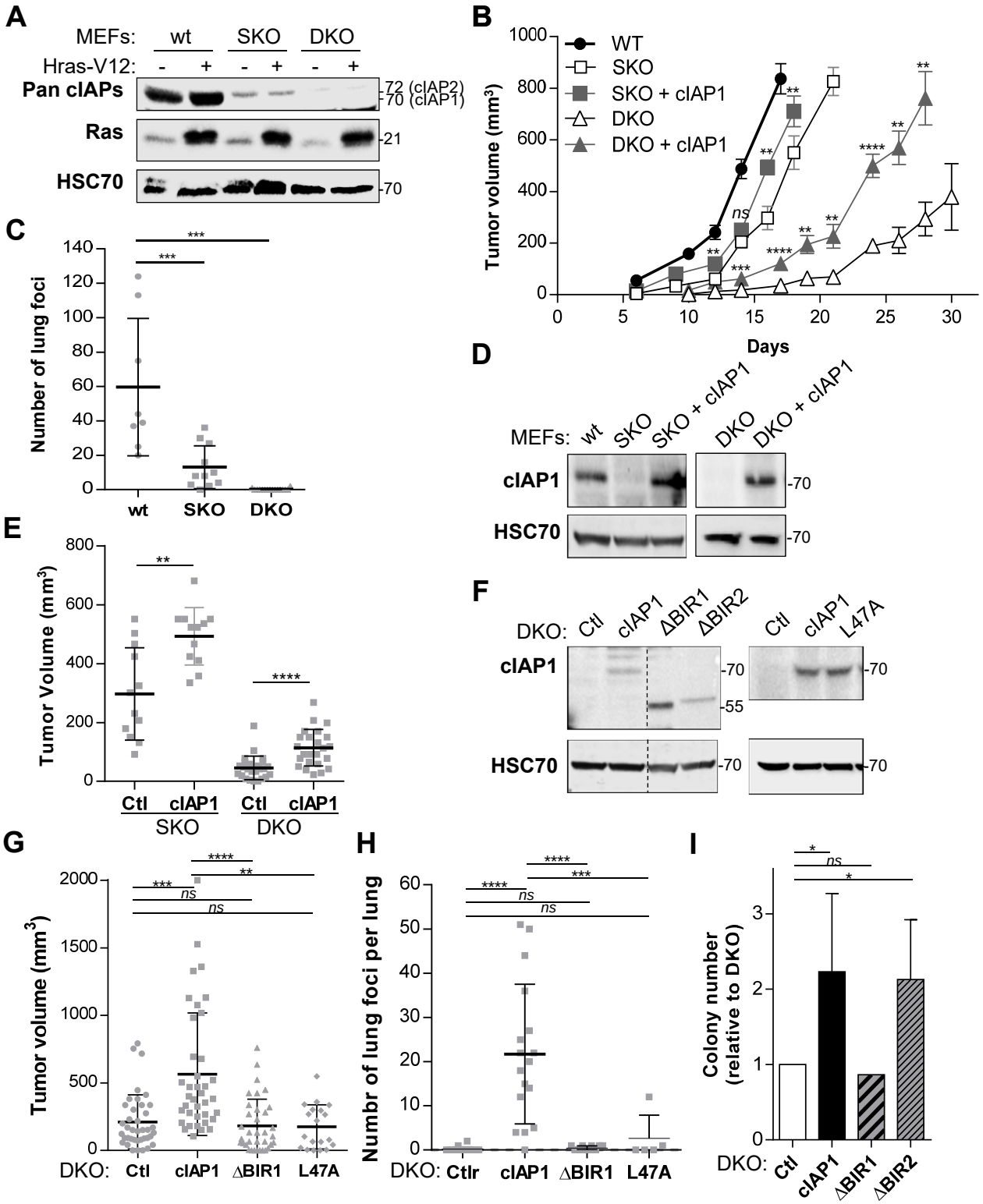

A
MEFs: wt SKO DKO
Hras-V12: - + - + - +
Pan cIAPs
Ras
HSC70
72 (cIAP2)
70 (cIAP1)
21
70
B
WT
SKO
SKO + cIAP1
DKO
DKO + cIAP1
Tumor volume (mm3)
Days
C
Number of lung foci
wt
SKO
DKO
D
MEFs: wt SKO SKO + cIAP1 DKO DKO + cIAP1
cIAP1
HSC70
E
Tumor Volume (mm3)
Ctl
cIAP1
SKO
DKO
F
DKO: Ctl cIAP1 ΔBIR1 ΔBIR2 Ctl cIAP1 L47A
cIAP1
HSC70
G
Tumor volume (mm3)
DKO: Ctl cIAP1 ΔBIR1 L47A
H
Numbr of lung foci per lung
DKO: Ctlr cIAP1 ΔBIR1 L47A
I
Colony number (relative to DKO)
DKO: Ctl cIAP1 ΔBIR1 ΔBIR2

FIGURE 2

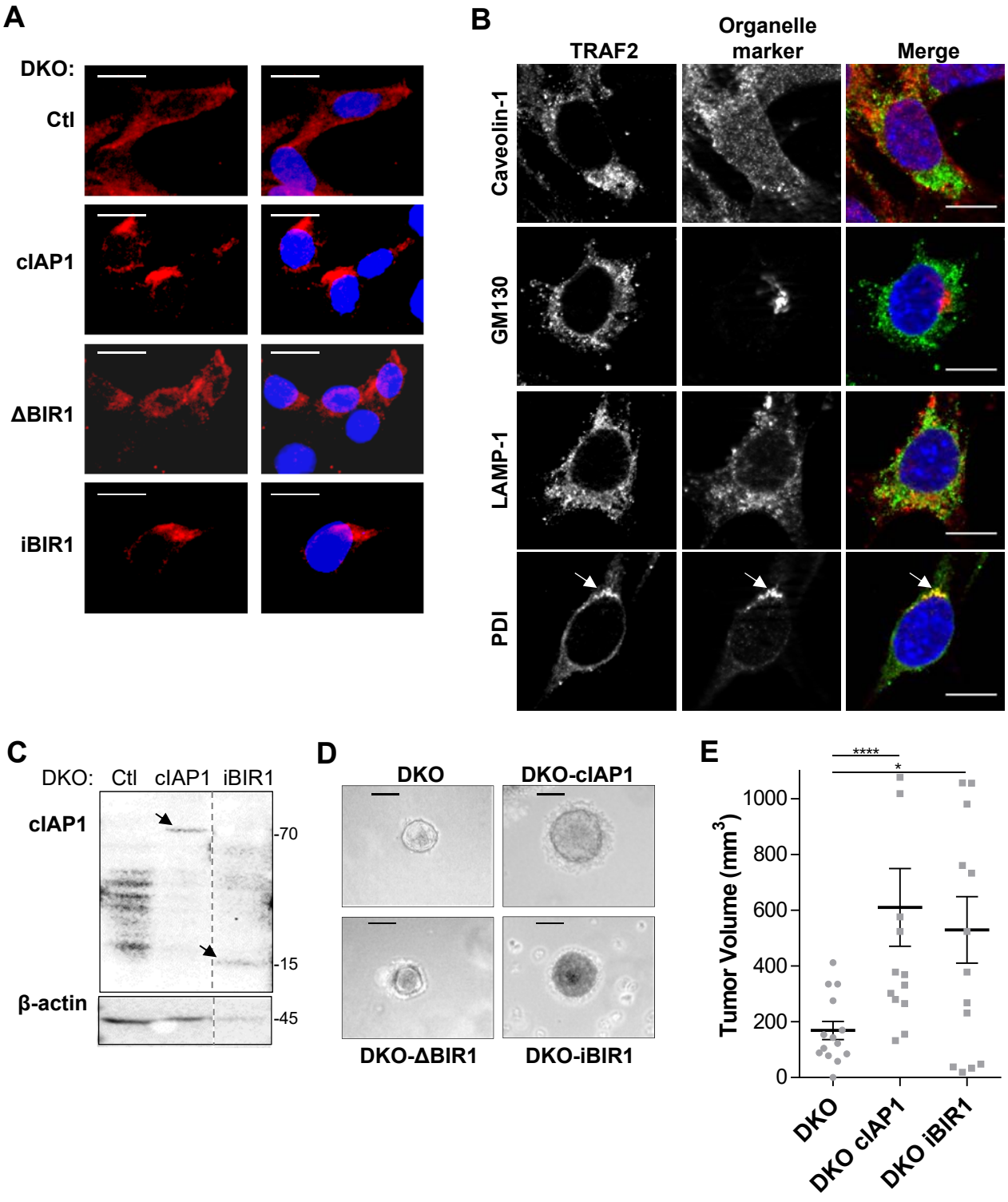
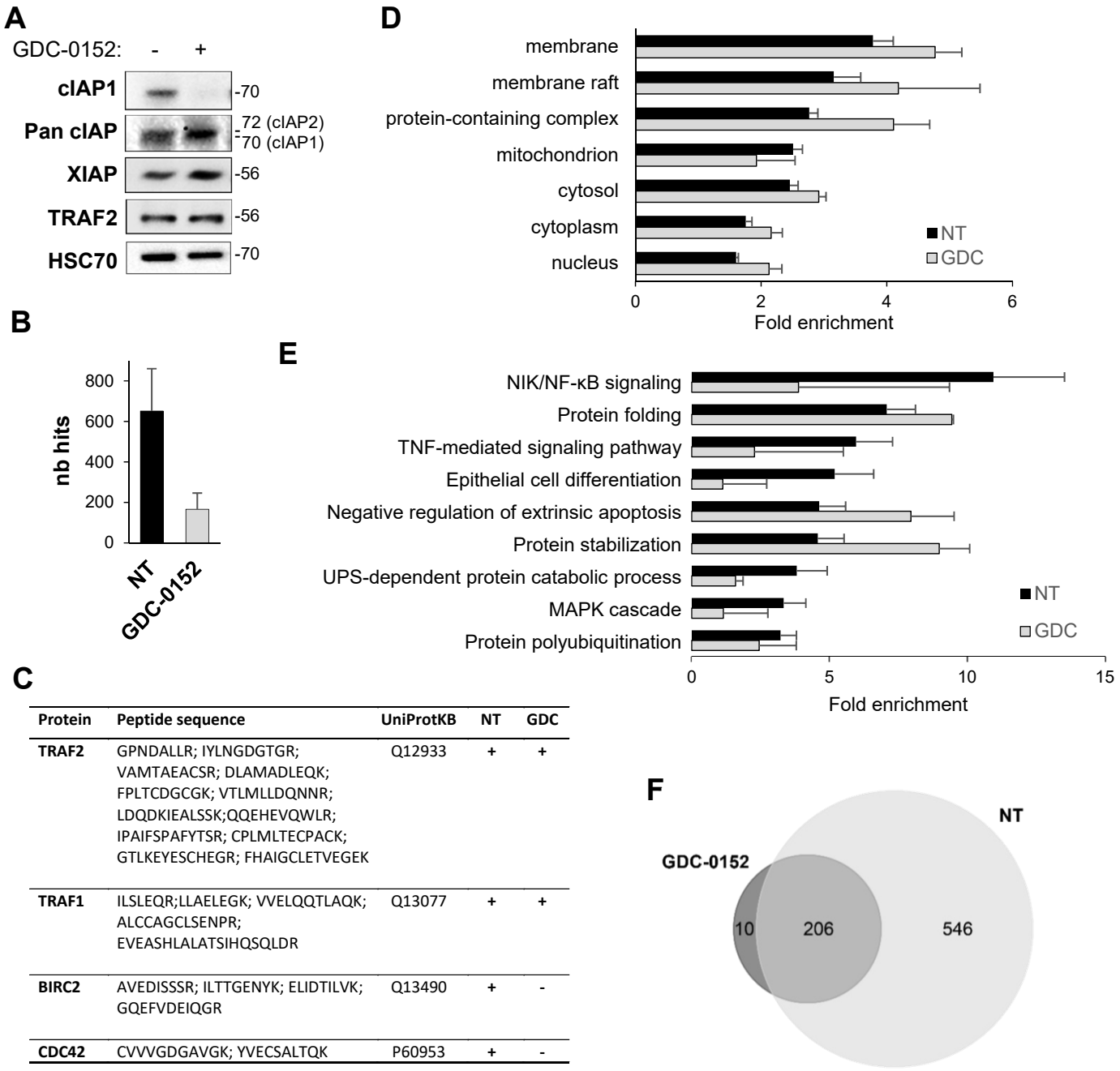

A
DKO:
Ctl
cIAP1
ΔBIR1
iBIR1
B
TRAF2
Organelle marker
Merge
Caveolin-1
GM130
LAMP-1
PDI
C
DKO: Ctl cIAP1 iBIR1
cIAP1
β-actin
-70
-15
-45
D
DKO
DKO-cIAP1
DKO-ΔBIR1
DKO-iBIR1
E
****
*
Tumor Volume (mm3)
1000
800
600
400
200
0
DKO
DKO cIAP1
DKO iBIR1

FIGURE 3



C

Protein	Peptide sequence	UniProtKB	NT	GDC
TRAF2	GPNDALLR; IYLNGDGTGR; VAMTAEACSR; DLAMADLEQK; FPLTCDGCGK; VTLMLLDQNNR; LDQDKIEALSSK;QQEHEVQWLR; IPAIFSPAFYTSR; CPLMLTECPACK; GTLKEYESCHEGR; FHAIGCLETVEGEK	Q12933	+	+
TRAF1	ILSLEQR;LLAELEGK; VVELQQTLAQK; ALCCAGCLSENPR; EVEASHLALATSIHQSQLDR	Q13077	+	+
BIRC2	AVEDISSSR; ILTTGENYK; ELIDTILVK; GQEFVDEIQGR	Q13490	+	-
CDC42	CVVVGDGAVGK; YVECSALTQK	P60953	+	-

FIGURE 4

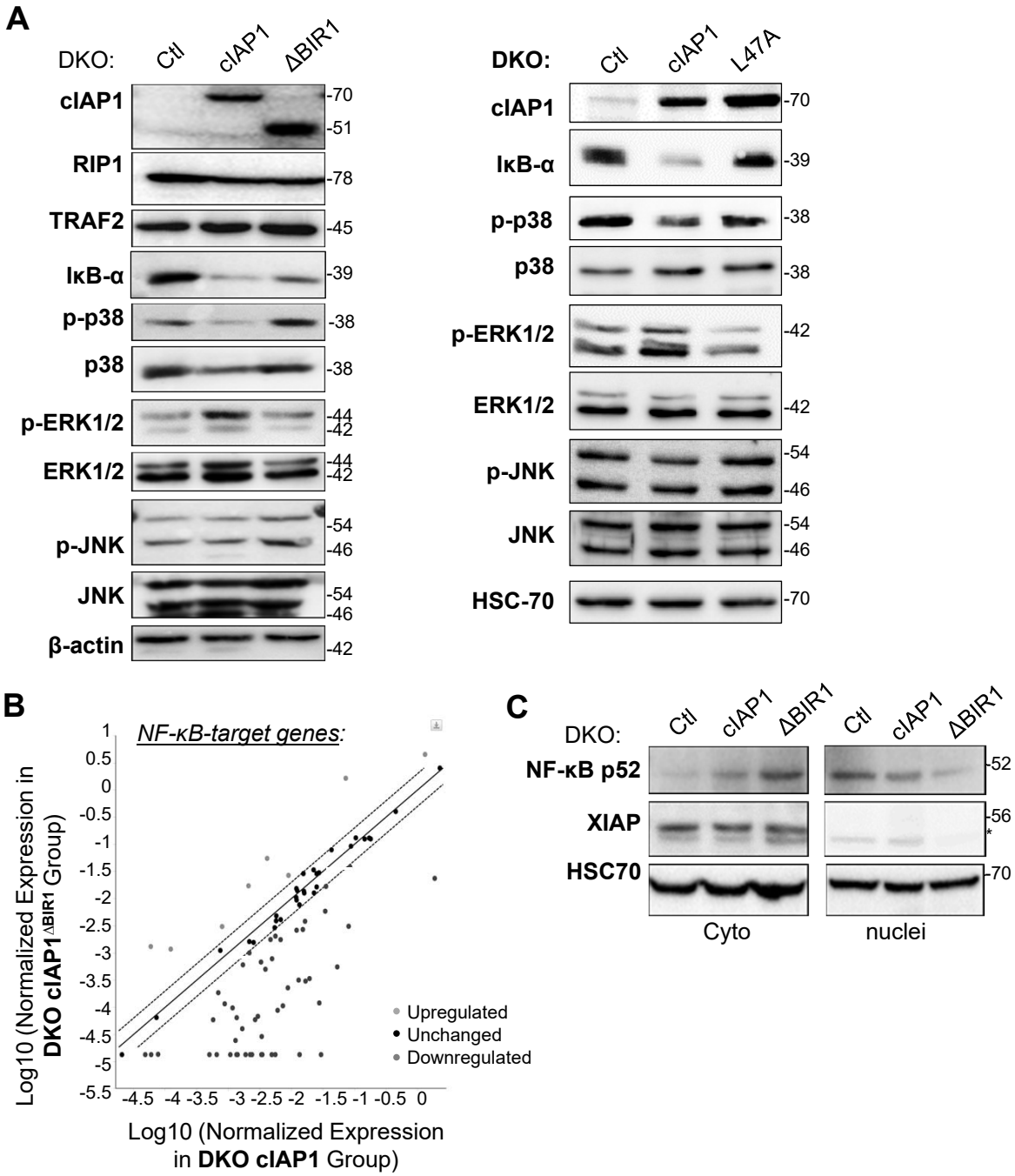

A
DKO:
Ctl
cIAP1
ΔBIR1
cIAP1
RIP1
TRAF2
IκB-α
p-p38
p38
p-ERK1/2
ERK1/2
p-JNK
JNK
β-actin
-70
-51
-78
-45
-39
-38
-38
-44
-42
-44
-42
-54
-46
-54
-46
-42
DKO:
Ctl
cIAP1
L47A
cIAP1
IκB-α
p-p38
p38
p-ERK1/2
ERK1/2
p-JNK
JNK
HSC-70
-70
-39
-38
-38
-42
-42
-54
-46
-54
-46
-70
B
NF-κB-target genes:
Log10 (Normalized Expression in DKO cIAP1ΔBIR1 Group)
Log10 (Normalized Expression in DKO cIAP1 Group)
Upregulated
Unchanged
Downregulated
C
DKO:
Ctl
cIAP1
ΔBIR1
Ctl
cIAP1
ΔBIR1
NF-κB p52
XIAP
HSC70
-52
-56
*
-70
Cyto
nuclei

FIGURE 5

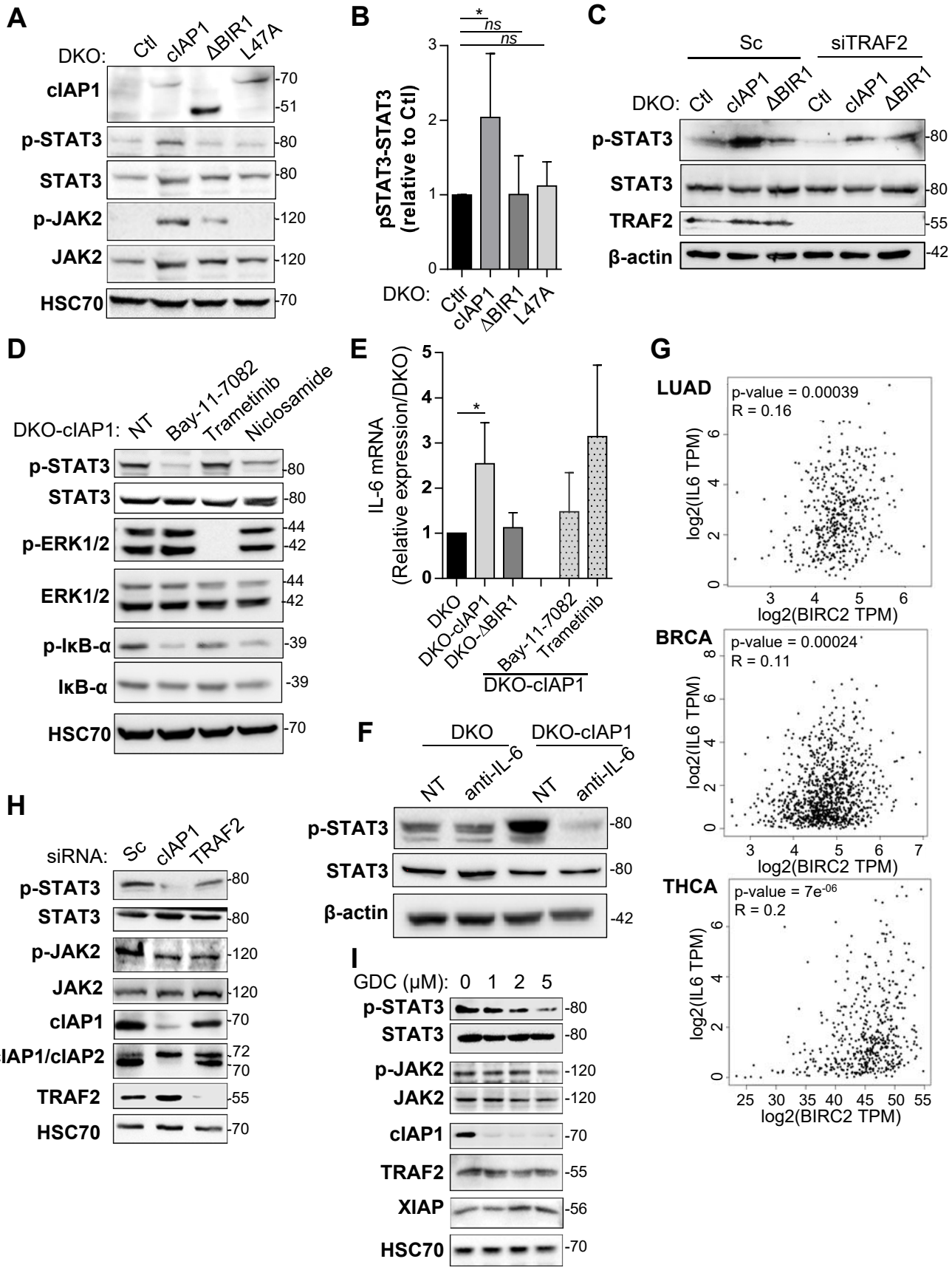
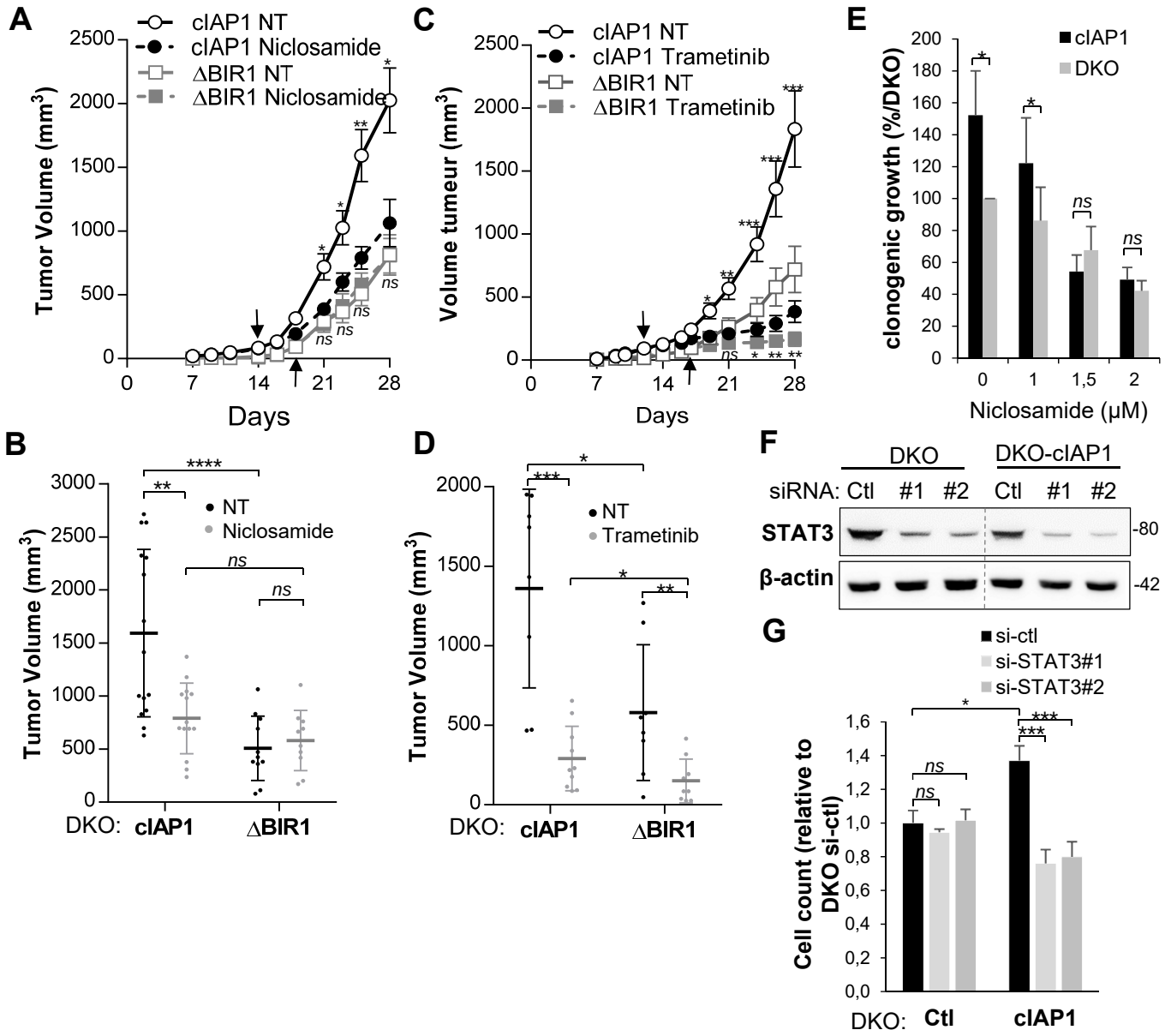

A
DKO:
Ctl
cIAP1
ΔBIR1
L47A
cIAP1
p-STAT3
STAT3
p-JAK2
JAK2
HSC70
B
pSTAT3-STAT3 (relative to Ctl)
*
ns
ns
DKO:
Ctlr
cIAP1
ΔBIR1
L47A
C
Sc
siTRAF2
DKO:
Ctl
cIAP1
ΔBIR1
Ctl
cIAP1
ΔBIR1
p-STAT3
STAT3
TRAF2
β-actin
D
DKO-cIAP1:
NT
Bay-11-7082
Trametinib
Niclosamide
p-STAT3
STAT3
p-ERK1/2
ERK1/2
p-IκB-α
IκB-α
HSC70
E
IL-6 mRNA (Relative expression/DKO)
*
DKO
DKO-cIAP1
DKO-ΔBIR1
Bay-11-7082
Trametinib
DKO-cIAP1
F
DKO
DKO-cIAP1
NT
anti-IL-6
NT
anti-IL-6
p-STAT3
STAT3
β-actin
G
LUAD
p-value = 0.00039
R = 0.16
log2(IL6 TPM)
log2(BIRC2 TPM)
BRCA
p-value = 0.00024
R = 0.11
log2(IL6 TPM)
log2(BIRC2 TPM)
THCA
p-value = 7e-06
R = 0.2
log2(IL6 TPM)
log2(BIRC2 TPM)
H
siRNA:
Sc
cIAP1
TRAF2
p-STAT3
STAT3
p-JAK2
JAK2
cIAP1
cIAP1/cIAP2
TRAF2
HSC70
I
GDC (μM): 0 1 2 5
p-STAT3
STAT3
p-JAK2
JAK2
cIAP1
TRAF2
XIAP
HSC70

FIGURE 6


A
cIAP1 NT
cIAP1 Niclosamide
ΔBIR1 NT
ΔBIR1 Niclosamide
Tumor Volume (mm3)
Days
C
cIAP1 NT
cIAP1 Trametinib
ΔBIR1 NT
ΔBIR1 Trametinib
Volume tumeur (mm3)
Days
E
cIAP1
DKO
clonogenic growth (%/DKO)
Niclosamide (µM)
B
NT
Niclosamide
Tumor Volume (mm3)
DKO: cIAP1 ΔBIR1
D
NT
Trametinib
Tumor Volume (mm3)
DKO: cIAP1 ΔBIR1
F
DKO
DKO-cIAP1
siRNA: Ctl #1 #2 Ctl #1 #2
STAT3
β-actin
-80
-42
G
si-ctl
si-STAT3#1
si-STAT3#2
Cell count (relative to DKO si-ctl)
DKO: Ctl cIAP1